ELSEVIER

Journal of Hazardous Materials B80 (2000) 189–206

Journal of Hazardous Materials

www.elsevier.nl/locate/jhazmat

Kinetic modelling of aqueous atrazine ozonation processes in a continuous flow bubble contactor

Fernando J. Beltrán*, Manuel González, Benito Acedo, Francisco J. Rivas

Departamento de Ingeniería Química y Energética, Universidad de Extremadura, 06071 Badajoz, Spain

Received 13 March 2000; received in revised form 24 July 2000; accepted 26 July 2000

Abstract

The ozonation of atrazine in different waters (ultrapure and surface waters) has been studied in continuous bubble contactors with kinetic modelling purposes. Three ozonation processes have been considered: ozonation alone and combined with hydrogen peroxide or UV radiation. The kinetic models are based on a molecular and free radical mechanism of reactions, reaction rate and mass transfer data and non-ideal flow analysis models for gas and water phases through the contactors (the tanks in series model and the dispersion model). The models predict well the experimental concentrations of atrazine, dissolved ozone and hydrogen peroxide both at non-steady state and steady state regimes. From both experimental and calculated results, atrazine conversions are observed to be highly dependent on the nature of water where ozonation is carried out. As far as removal of atrazine and oxidation intermediates are concerned, ozone combined with UV radiation resulted in the most effective ozonation process among the three studied.

Keywords: Kinetic modelling; Ozonation processes; Atrazine; Hydrogen peroxide; UV radiation

1. Introduction

Atrazine is one of the most widely used herbicides in agriculture and, as a consequence, its presence in aquatic environments has been extensively reported previously [1,2]. Among herbicides, atrazine presents a high solubility in water and its concentration in natural waters has very often been found above the maximum permissible level: 0.1 $\mu g\,l^{-1}$ according to EC

Abbreviations: A, atrazine; DEA, deethylatrazine; DIA, deisopropylatrazine; DEIA, deethyldeisopropylatrazine; g, gas phase; L, water phase; 0, conditions at time zero; RTDF, residence time distribution function

*Corresponding author. Tel.: +34-24-28-9387; fax: +34-24-27-1304.
E-mail address: fbeltran@unex.es (F.J. Beltrán).

0304-3894/00/$ – see front matter
PII: S0304-3894(00)00302-2

Directives [3]. Nonetheless, removal of atrazine by chemical treatments has been shown to be a suitable and effective technology to meet all federal, state and local discharge regulations [4].

Ozonation of atrazine in water has already been studied by different authors and, subsequently, data on intermediate formation, rate constant calculations and process modelling have been reported [4–9]. Nevertheless, most studies published on this subject have been completed by means of experiments conducted in semibatch reactors with the herbicide dissolved in ultrapure or well-defined laboratory prepared water. In some other cases, the kinetic modelling has been limited to ozonation alone or combined with hydrogen peroxide without studying the actual characteristics of the gas flow through the ozonation column [10].

It is known that main disappearance route of atrazine when using ozone, hydrogen peroxide and/or UV radiation goes through a mechanism of molecular compounds and free radicals generated in the process [8,11]. Thus, the presence of other substances in this type of treatment may significantly influence atrazine and intermediates removal rate depending on the initiating, promoting or inhibiting free radical character of these compounds [12].

In this paper, a kinetic model has been applied to three ozonation processes (ozonation alone and combined with hydrogen peroxide or UV radiation) of atrazine carried out in a continuous regime for both the gas and water phases. The kinetics have been completed with information on the non-ideal flow characteristics of gas and water phases through the ozonation contactors by the use of the tanks in series and dispersion models [13].

2. Experimental procedures

Experiments were carried out in two ozonation bubble contactors (see Table 1 for dimensions). One of them aimed at completing UV radiation experiments (contactor I), was a photochemical reactor consisting of a bubble column with a quartz well placed along the central axis. Both contactors were equipped with a porous plate at their bottom through which the oxidising gas (oxygen–ozone) was fed countercurrently to the water phase containing the herbicide. The water flow rate varied depending on the contactor used (see Table 1), so that the hydraulic residence time was always 10 min, a typical value in real ozonation contactors [14]. A 15 W Hanau low pressure mercury vapor lamp was situated in the quartz well for UV radiation experiments.

Two different surface waters located in the Province of Badajoz (south west of Spain) were used in this study. Their main characteristics are presented in Table 2. The surface water was allowed to settle down for 24 h and filtered through a 0.45 μm Millipore membrane before

Table 1
Dimensions and flow rates for the contactors used in this work

Contactors	Height (cm)	Diameter (cm)	Gas flowrate ($l\,h^{-1}$)	Liquid flowrate ($l\,min^{-1}$)
Photochemical (I)	32.5	9.00	20	0.195
Non-photochemical (II)	181.5	4.15	20	0.250

Table 2
Characteristics of surface waters used in this work

	Cordobilla reservoir	Gévora river
pH	8.1	7.9
Chemical oxygen demand ($mg\,l^{-1}$)	9.4	8.5
Total carbon ($mg\,l^{-1}$)	33.7	20.1
Inorganic carbon ($mg\,l^{-1}$)	5.76	8.6
Absorbance at 254 nm	0.109	0.124

use. In addition, some experiments were carried out in ultrapure water (Milli Q Millipore system) for comparative purposes.

Atrazine was obtained from 'Dr. Ehrenstorfer laboratory' (D 86199 Augsburg, Germany) and used as received. Aqueous solutions of atrazine were prepared from a saturated one of the herbicide in water. Thereby, an excess amount of atrazine was first added to the bulk water and after 24 h agitation in the dark, filtered through 0.45 μm Millipore membranes and analysed.

Ozone was produced from pure oxygen in a laboratory ozonator able to generate a maximum of 4 g Ozone h^{-1}. Atrazine was analysed by means of high performance liquid chromatography (HPLC) using a 150 mm × 4.6 mm C-Supelcosil LC-8 column and a 486 Waters UV/Visible detector set at 214 nm. The mobile phase was an acetonitrile–water mixture (30:70, v/v) and the system operated in isocratic mode. Ozone in the gas phase was analysed with a GM19 Anseros analyser. Aqueous ozone concentration was determined by the indigo method [15]. Low hydrogen peroxide concentrations were determined by means of a modified fluorescence method [16].

Determination of non-ideal flow data was accomplished by tracer experiments [13]. For the aqueous phase, methylene blue was used as a tracer and pulse input was chosen as the injection mode. For the gas phase, ozone was the tracer and used in the negative step mode of injection. In these experiments ozone decomposition was avoided by adjusting the pH of the aqueous medium below 2.

The volumetric mass transfer coefficient, $k_L a$, was determined from physical ozone absorption experiments in water following a well-known method already reported in the literature [17]. For absorption experiments completed at pH above 2, parallel runs were carried out using oxygen instead of ozone. Results obtained, once oxygen and ozone diffusivities were accounted for, were similar. Average values of 3.7×10^{-3} and $4.3 \times 10^{-3}\,s^{-1}$, were found for $k_L a$ of the contactors I and II, respectively. Hydrogen peroxide was used for actinometric experiments to determine the intensity of incident radiation and the effective path of radiation through the photoreactor (contactor I), that were found to be 1.91×10^{-6} Einstein $l^{-1}\,s^{1}$ and 6.6 cm, respectively.

3. Results and discussion

Chemical oxidation of atrazine (A) leads to the formation of a series of intermediates which are also simultaneously degraded to finally yield cyanuric acid [7]. In this work,

deethylatrazine (DEA), desisopropylatrazine (DIA) and deethyldeisopropylatrazine (DEIA) were assumed to be the main compounds formed at the beginning of the ozonation process. Although, atrazine ozonation mainly develops through hydroxyl radical oxidation in the mechanism that follows the direct reaction with ozone has also been included. The molecular and free radical mechanism presented in Eqs. (1)–(26) has been considered to model the oxidation of atrazine and corresponding intermediates.

The proposed mechanism is based on the reported works [1,4,7,18,19]. The following set of reactions was considered to describe the ozonation processes of atrazine and main by-products.

1. Direct reactions:

$$O_3 + A \rightarrow z_{DE}\ DEA \qquad k_{D,A} = 6\,M^{-1}\,s^{-1} \tag{1}$$

$$O_3 + A \rightarrow z_{DI}\,DIA \qquad k_{D,A} = 6\,M^{-1}\,s^{-1} \tag{2}$$

$$O_3 + DEA \rightarrow 0.5\,DEIA \qquad k_{D,DEA} = 0.2\,M^{-1}\,s^{-1} \tag{3}$$

$$O_3 + DIA \rightarrow 0.5\,DEIA \qquad k_{D,DIA} = 7.5\,M^{-1}\,s^{-1} \tag{4}$$

$$O_3 + DEIA \rightarrow P \qquad k_{D,DEIA} = 0.2\,M^{-1}\,s^{-1} \tag{5}$$

$$O_3 + H_2O + h\nu \rightarrow H_2O_2 \qquad \phi_{O_3} = 0.64\,\text{mol photon}^{-1} \tag{6}$$

$$A + h\nu \rightarrow \text{Products} \qquad \phi_A = 0.05\,\text{mol photon}^{-1} \tag{7}$$

$$DEA + h\nu \rightarrow \text{Products} \qquad \phi_{O_3} = 0.035\,\text{mol photon}^{-1} \tag{8}$$

$$DIA + h\nu \rightarrow \text{Products} \qquad \phi_{O_3} = 0.038\,\text{mol photon}^{-1} \tag{9}$$

$$DEIA + h\nu \rightarrow \text{Products} \qquad \phi_{O_3} = 0.018\,\text{mol photon}^{-1} \tag{10}$$

2. Free radical initiation reactions.

$$O_3 + OH^- \rightarrow {}^\bullet HO_2 + {}^\bullet O_2{}^- \qquad k_{i1} = 70\,M^{-1}\,s^{-1} \tag{11}$$

$$O_3 + HO_2{}^- \rightarrow {}^\bullet HO_2 + {}^\bullet O_3{}^- \qquad k_{i2} = 2.8 \times 10^6\,M^{-1}\,s^{-1} \tag{12}$$

$$H_2O_2 + h\nu \rightarrow 2{}^\bullet OH \qquad \phi_{O_3} = 0.5\,\text{mol photon}^{-1} \tag{13}$$

$$O_3 + In \rightarrow In^+ + {}^\bullet O_3{}^- \qquad k_{In} \tag{14}$$

where In represents any possible radical chain initiating species present in water.

3. Free radical propagation reactions:

$${}^\bullet HO_2 \leftrightarrow {}^\bullet O_2{}^- + H^+ \qquad pK = 4.8 \tag{15}$$

$$O_3 + {}^\bullet O_2{}^- \rightarrow O_2 + {}^\bullet O_3{}^- \qquad k_{p1} = 1.6 \times 10^9\,M^{-1}\,s^{-1} \tag{16}$$

$${}^\bullet O_3{}^- + H^+ \rightarrow {}^\bullet HO_3 \qquad k_{p2} = 5 \times 10^{10}\,M^{-1}\,s^{-1} \tag{17}$$

$${}^\bullet HO_3 \rightarrow {}^\bullet OH + O_2 \qquad k_{p3} = 1.4 \times 10^5\,s^{-1} \tag{18}$$

$$H_2O_2 + {}^{\bullet}OH \rightarrow {}^{\bullet}HO_2 + H_2O \qquad k_{p4} = 2.7 \times 10^7\ M^{-1}\ s^{-1} \tag{19}$$

$$HO_2{}^- + {}^{\bullet}OH \rightarrow {}^{\bullet}HO_2 + OH^- \qquad k_{p5} = 7.5 \times 10^9\ M^{-1}\ s^{-1} \tag{20}$$

$$HCO_3{}^- + {}^{\bullet}OH \rightarrow {}^{\bullet}CO_3{}^- + H_2O \qquad k_{p6} = 2 \times 10^7\ M^{-1}\ s^{-1} \tag{21}$$

$$CO_3{}^{2-} + {}^{\bullet}OH \rightarrow {}^{\bullet}CO_3{}^- + OH^- \qquad k_{p7} = 3.7 \times 10^8\ M^{-1}\ s^{-1} \tag{22}$$

$${}^{\bullet}CO_3{}^- + H_2O_2 \rightarrow HCO_3{}^- + {}^{\bullet}HO_2 \qquad k_{p8} = 8 \times 10^5\ M^{-1}\ s^{-1} \tag{23}$$

$${}^{\bullet}CO_3{}^- + HO_2{}^- \rightarrow CO_3{}^{2-} + {}^{\bullet}HO_2 \qquad k_{p9} = 5.6 \times 10^7\ M^{-1}\ s^{-1} \tag{24}$$

$$A + {}^{\bullet}OH \rightarrow {}^{\bullet}R + z_{RE}\,DEA \qquad k_{OH,A} = 1.8 \times 10^{10}\ M^{-1}\ s^{-1} \tag{25}$$

$$A + {}^{\bullet}OH \rightarrow {}^{\bullet}R + z_{RI}\,DIA \qquad k_{OH,A} = 1.8 \times 10^{10}\ M^{-1}\ s^{-1} \tag{26}$$

$$DEA + {}^{\bullet}OH \rightarrow {}^{\bullet}R + 0.5\,DEIA \qquad k_{OH,DEA} = 2 \times 10^9\ M^{-1}\ s^{-1} \tag{27}$$

$$DIA + {}^{\bullet}OH \rightarrow {}^{\bullet}R + 0.5\,DEIA \qquad k_{OH,DIA} = 2.1 \times 10^9\ M^{-1}\ s^{-1} \tag{28}$$

$$DEIA + {}^{\bullet}OH \rightarrow {}^{\bullet}R + P \qquad k_{OH,DEA} = 4.8 \times 10^8\ M^{-1}\ s^{-1} \tag{29}$$

$${}^{\bullet}R + O_2 \rightarrow {}^{\bullet}ROO \rightarrow {}^{\bullet}O_2{}^- + P \qquad k_{p10} \tag{30}$$

4. Free radical termination reactions:

$$OM + {}^{\bullet}OH \rightarrow P \qquad k_{t1} \tag{31}$$

$${}^{\bullet}CO_3{}^- + OM \rightarrow P \qquad k_{t2} \tag{32}$$

where OM stands for the organic matter content of the surface water in which atrazine is dissolved. In addition, chemical equilibria in water of hydrogen peroxide, carbonic and phosphoric acids were also considered.

In these equations z_{DE}, z_{DI}, z_{RE} and z_{RI} represent the stoichiometric coefficients of decomposition of atrazine to form DEA and DIA either by direct reaction with ozone or with the hydroxyl radical, respectively. These values were found to be 0.033, 0.039, 0.14 and 0.06 for reactions (1), (2), (25) and (26), respectively [4]. Finally, Table 3 shows values of the extinction coefficients at 254 nm (ε_i) for the compounds present in the kinetic model.

At the conditions used in this study all the ozone involving reactions above indicated were found to develop in the slow regime [17] and, thereby, chemical reactions controlled the overall kinetics of the process.

Table 3
Extinction coefficients of compounds considered in the kinetic model[a]

Compound	ε ($M^{-1}\,s^{-1}$)	Compound	ε ($M^{-1}\,s^{-1}$)
O_3	3300	DEIA	3161
A	2487	H_2O_2	19
DEA	3291	$HO_2{}^-$	210
DIA	3056		

[a] Values taken from Beltrán et al. [4,8,11].

Thus, the kinetic expression describing the ozone absorption rate would be:

$$N_{O_3} = k_L a(C^*_{O_3} - C_{O_3}) = k_L a\left(C_g \frac{RT}{He} - C_{O_3}\right) \quad (33)$$

where $k_L a$ is the individual mass transfer coefficient in the liquid phase, *He* the Henry's constant, $C^*_{O_3}$ the ozone concentration at the gas–liquid interphase, C_g the ozone concentration in the gas phase, C_{O_3} the ozone concentration in the liquid and *R* and *T* the universal gas constant and temperature, respectively.

The chemical reaction rate equations in water for the main chemical species were then derived from Eqs. (1)–(32). These equations are given.

For ozone:

$$r_{O_3} = \left(\sum_i k_{D,i}C_i + k_{i1}C_{OH^-} + k_{i2}C_{HO_2^-} + k_i C_i + k_{p1}C_{\bullet O_2^-} + k_{in}C_{in}\right) C_{O_3} \quad (34)$$

For atrazine:

$$-r_A = k_{D,A}C_A C_{O_3} + k_{OH,A}C_A C_{\bullet OH} \quad (35)$$

For DEA:

$$r_{DEA} = (z_{DE}k_{D,A}C_A - k_{D,DEA}C_{DEA})C_{O_3} + (z_{RE}k_{OH,A}C_A - k_{OH,DEA}C_{DEA})C_{\bullet OH} \quad (36)$$

For DIA:

$$r_{DIA} = (z_{DI}k_{D,A}C_A - k_{D,DIA}C_{DIA})C_{O_3} + (z_{RI}k_{OH,A}C_A - k_{OH,DIA}C_{DIA})C_{\bullet OH} \quad (37)$$

For DEIA:

$$r_{DEIA} = (0.5(k_{D,DEA}C_{DEA} + k_{D,DIA}C_{DIA}) - k_{D,DEIA}C_{DEIA})C_{O_3} + (0.5(k_{OH,DEA}C_{DEA} + k_{OH,DIA}C_{DIA}) - k_{OH,DEIA}C_{DEIA})C_{\bullet OH} \quad (38)$$

For hydrogen peroxide:

$$r_{H_2O_{2T}} = \left(\sum_i (k_{OH,i}C_i) - k_H C_{H_2O_{2T}}\right) C_{\bullet OH} - k_{i2}C_{HO_2^-}C_{O_3} - k_C C_{H_2O_{2T}}C_{O_3} \quad (39)$$

Carbonates:

$$r_{HCO_{3T}} = k_C C_{H_2O_{2T}} C_{\bullet CO_3} - k_S C_{H_2CO_{3T}} \quad (40)$$

where

$$k_S = [k_{p6} + k_{p7}10^{pH-10.25}]\frac{10^{pH-6.37}}{1 + 10^{pH-6.37} + 10^{2pH-16.32}} \quad (41)$$

$$k_C = \frac{k_{p8} + k_{p9}10^{pH-11.8}}{1 + 10^{pH-11.8}} \quad (42)$$

and

$$k_{\mathrm{H}} = \frac{k_{p4} + k_{p5} 10^{\mathrm{pH}-11.8}}{1 + 10^{\mathrm{pH}-11.8}} \tag{43}$$

In the case UV radiation is also applied, another decomposition rate term due to direct photolysis has to be added to the right-hand side of Eqs. (34)–(39). This contribution takes the following form:

$$r_{\mathrm{UV}i} = I_0 \phi_i F_i \exp(-2.303\, L \sum \varepsilon_i C_i) \tag{44}$$

where I_0 and L represents the intensity of incident radiation and effective path of radiation through the photoreactor, and F_i the fraction of radiation the species i absorbs, defined as follows:

$$F_i = \frac{\varepsilon_i C_i}{\sum \varepsilon_j C_j} \tag{45}$$

where ε_i and ε_j are the extinction coefficients at 254 nm of species i and j, respectively.

In Eq. (34), the term $k_{\mathrm{In}} C_{\mathrm{In}} C_{\mathrm{O_3}}$ represents the contribution of some substances initially present in water to decompose ozone in free radicals through reaction (13). Values of the term $k_{\mathrm{In}} C_{\mathrm{In}}$ were estimated from experiments of ozone decomposition in the three waters studied by assuming a pseudo first order kinetics. Thus, these rate constant values were found to be 3.75×10^{-4}, 3.72×10^{-3} and $2.38 \times 10^{-3}\ \mathrm{s}^{-1}$ for the ozone decomposition in ultrapure, Cordobilla and Gevora waters, respectively.

3.1. Kinetic model

The kinetic model was proposed taking into account both the kinetic information given in the mechanism of reactions and the residence time distribution function (RTDF) obtained by tracer analysis in the gas and liquid phases [13]. Data of non-ideal flow analysis are given in Table 4. From these results it is concluded that, at the conditions investigated, the flow of water through both contactors behaves in a different way. Thus, according to the tanks in series model, both the water and gas flows are perfectly mixed in the photochemical contactor. In the non-photochemical contactor, the gas flow is also perfectly mixed but the water flow has to be simulated with four ideal continuous stirred tanks of equal volume. Table 4, also presents the corresponding Peclet numbers for both gas and water flows

Table 4
Parameters of non-ideal flow analysis for the photochemical (I) and non-photochemical (II) contactors[a]

Contactor	Water phase					Gas phase			
	τ (min)	t_{m} (min)	σ^2 (min^2)	N	Pe	t_{m} (min)	σ^2 (min^2)	N	Pe
(I)	10	8.42	70.11	1.01	0.0325	2.96	4.50	1.95	2.43
(II)	10	8.99	21.54	3.76	6.3300	3.55	7.88	1.60	1.61

[a] τ: hydraulic time; t_{m}: residence time; σ^2: time distribution variance; N: number of continuous perfectly mixed tanks in series; Pe: Peclet number.

through both contactors. These values were later used to apply the dispersion model to the experimental results of atrazine ozonation processes.

3.1.1. The perfectly mixed tanks in series model

Mole balance equations of species in water were applied to each of the assumed ideal tanks that simulated the water flow. The equations for the *i*th tank are shown below.

1. For ozone in water:

$$Q_L(C_{O_3 i} - C_{O_3}) + (r_{O_3} + N_{O_3})\beta\Delta V = \frac{dC_{O_3}}{dt}\beta\Delta V \tag{46}$$

where Q_L is the water flow rate, $C_{O_3 i}$ and C_{O_3} the inlet and outlet ozone concentrations in water in the *i*th reactor considered, respectively, r_{O_3} the ozone chemical reaction rate, N_{O_3} the ozone absorption rate, β the liquid fraction in the reactor and ΔV is the reactor volume, defined as

$$\Delta V = \frac{V}{N} \tag{47}$$

V and N being the total contactor volume and number of ideal tanks that simulate the water flow.

2. For the rest of species *j* in the water phase.

$$Q_L(C_{ji} - C_j) + r_j\beta\Delta V = \frac{dC_j}{dt}\beta\Delta V \tag{48}$$

To Eqs. (46) and (48) the ozone mole balance equation in the gas phase has to be added. In this case the ozone concentration at the contactor outlet is the same as that inside the contactor. The following expression applies.

3. For ozone in the gas phase:

$$Q_G(C_{gi} - C_g) - V(1-\beta)r_{O_3 g} - k_L a\beta V \sum \left(C_g \frac{RT}{He} - C_{O_3}\right) = \frac{dC_g}{dt} V(1-\beta) \tag{49}$$

where Q_G is the gas flow rate, C_{gi} and C_g the inlet and outlet ozone concentrations in the gas phase, respectively, and $r_{O_3 g}$ the ozone decomposition rate due to direct photolysis in the gas phase, defined as follows [9]:

$$r_{O_3 g} = I_0 \phi_{O_3 g} \tag{50}$$

where $\phi_{O_3 g}$ is the quantum yield of ozone photolysis in the gas that can be obtained from literature [20].

The set of first order differential Eqs. (46), (48) and (49) was solved by means of the 4th order Runge–Kutta method to yield the time concentration profiles of species in water. The initial conditions were as follows:

$$t = 0, \quad C_g = 0; \quad i = 1 \text{ to } N, \quad C_{O_3 i} = 0; \quad j = 1 \text{ to } 6, \quad C_{ji} = C_{ji0} \tag{51}$$

In Eq. (51) subscripts 1 to 6 corresponds to atrazine, DEA, DIA, DEIA, hydrogen peroxide and carbonates, respectively.

3.1.2. The dispersion model

In this model, convection and diffusion contribute to chemical species transport. Thereby the following equations describe the ozonation process in the bubble contactor:

1. For ozone in the water:

$$\beta SH\frac{\partial C_{O_3}}{\partial t} = D_{O_3}\frac{\partial^2 C_{O_3}}{\partial h^2} - u_L\frac{\partial C_{O_3}}{\partial h} + r_{O_3} + N_{O_3} \tag{52}$$

where D_{O_3} represents the ozone diffusivity and u_L the superficial velocity of the water.

2. For chemical species j (atrazine and intermediates, hydrogen peroxide and carbonates) in water:

$$\beta V\frac{\partial C_j}{\partial t} = D_j\frac{\partial^2 C_j}{\partial h^2} - u_L\frac{\partial C_j}{\partial h} + r_j \tag{53}$$

D_j being the diffusivity of the j species.

3. For ozone in the perfectly mixed gas phase:

$$(1-\beta)V\frac{dC_g}{dt} = Q_G(C_{gi} - C_g) - \beta k_L a\int_0^H \left(C_g\frac{RT}{He} - C_{O_3}\right) S\,dh - (1-\beta)Vr_{O_3g} \tag{54}$$

where H, S and dh represent the height, transversal area and differential height of the contactor, respectively.

By considering steady-state regime, Eqs. (52)–(54) become in dimensionless form as follows:

- For ozone in water:

$$\frac{1}{Pe_L}\frac{d^2\psi_{O_3}}{d\lambda^2} - \frac{d\psi_{O_3}}{d\lambda} + \tau_L\left[\frac{\omega_{O_3}}{C_{gi}} + k_L a\left(\psi_g\frac{RT}{He} - \psi_{O_3}\right)\right] = 0 \tag{55}$$

- For the chemical species j in water:

$$\frac{1}{Pe_L}\frac{d^2\psi_j}{d\lambda^2} - \frac{d\psi_j}{d\lambda} + \tau_L\frac{\omega_j}{C_{1,0}} = 0 \tag{56}$$

- For ozone in the gas phase:

$$\psi_g + \frac{\beta k_L a}{\tau_G}\int_0^1 \left(\psi_g\frac{RT}{He} - \psi_{O_3}\right) d\lambda = 1 \tag{57}$$

where

$$\psi_g = \frac{C_g}{C_{gi}} \tag{58}$$

$$\psi_{O_3} = \frac{C_{O_3}}{C_{gi}} \tag{59}$$

$$\psi_j = \frac{C_j}{C_{1,0}} \tag{60}$$

$$\lambda = \frac{h}{H} \tag{61}$$

$$Pe_{\mathrm{L}} = \frac{u_{\mathrm{L}} H}{D_j} \tag{62}$$

$\omega_{\mathrm{O_3}}$ and ω_j being the chemical reactions rates expressed as a function of $\psi_{\mathrm{O_3}}$ and ψ_j, respectively, and rate constants.

Now, Eqs. (55) and (56) can be transformed into a set of non-linear first order ordinary differential equations by defining the following functions:

$$\xi_{\mathrm{O_3}} = \frac{\mathrm{d}\psi_{\mathrm{O_3}}}{\mathrm{d}\lambda} \tag{63}$$

and

$$\xi_j = \frac{\mathrm{d}\psi_j}{\mathrm{d}\lambda} \tag{64}$$

thus, from Eqs. (63) and (64) it is obtained:

$$\frac{1}{Pe_{\mathrm{L}}} \frac{\mathrm{d}\xi_{\mathrm{O_3}}}{\mathrm{d}\lambda} - \xi_{\mathrm{O_3}} + \tau_{\mathrm{L}} \left[\frac{\omega_{\mathrm{O_3}}}{C_{\mathrm{gi}}} + k_{\mathrm{L}} a \left(\psi_{\mathrm{g}} \frac{RT}{He} - \psi_{\mathrm{O_3}} \right) \right] = 0 \tag{65}$$

$$\frac{1}{Pe_{\mathrm{L}}} \frac{\mathrm{d}\xi_j}{\mathrm{d}\lambda} - \xi_j + \tau_{\mathrm{L}} \frac{\omega_j}{C_{1,0}} = 0 \tag{66}$$

The system of first order differential Eqs. (63)–(66) was solved by following the flow diagram presented in Fig. 1 using a computer program (Mathematica for Windows, enhanced version 2.2) with the initial limiting conditions:

$$\begin{aligned} &\lambda = 0; \quad \psi_{\mathrm{g}} = \text{assumed}; \quad \psi_{\mathrm{O_3}} = 0; \quad j = 1 \text{ to } 6; \\ &\xi_j = 0; \quad \psi_1 = 1; \; j = 2 \text{ to } 6; \quad \psi_j = \frac{C_{j,0}}{C_{1,0}} \end{aligned} \tag{67}$$

For ψ_{g}, it was first assumed the value corresponding to the experimental measurement of C_{g} at the reactor outlet. Once the values of $\psi_{\mathrm{O_3}}$ and ψ_j in water at the column outlet were obtained, Eq. (57) was used to confirm the assumed value of ψ_{g}.

3.2. Simulation results

3.2.1. Ozonation alone

Ozonation results of atrazine in ultrapure water and surface water were first simulated with both kinetic models derived from the application of non-ideal fluid flow analysis. Fig. 2 presents an example of the results obtained. It shows the evolution of both experimental and calculated (with the tanks in series model) concentrations of atrazine with time corresponding to ozonation experiments in different waters. As can be seen, the type of water results fundamental to slow down or accelerate the oxidation rate. This confirms the nature of the ozonation process which is highly dependent on the presence of substances that

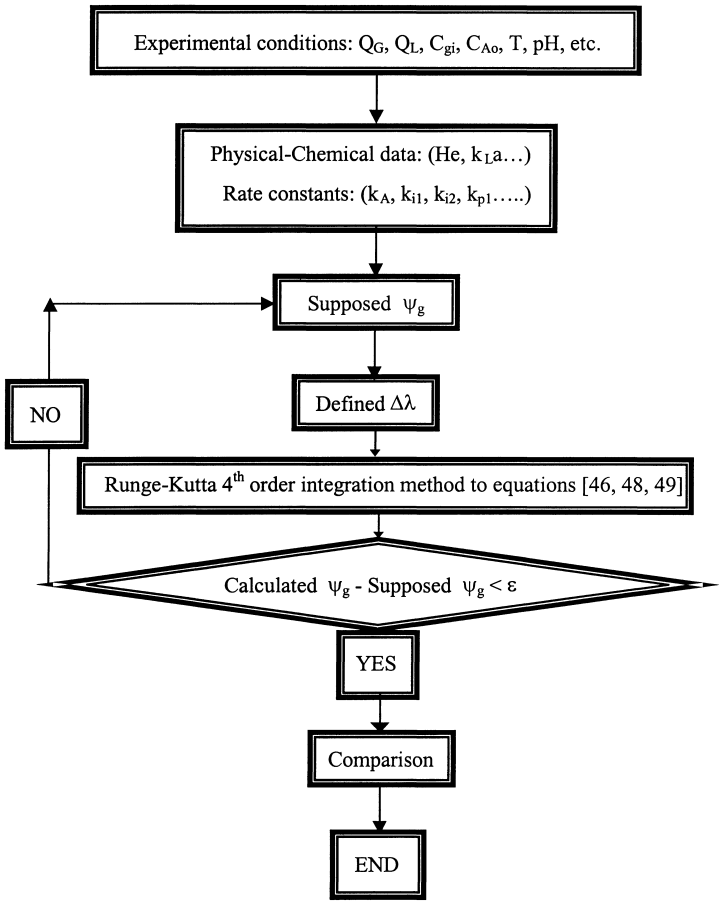

Fig. 1. Flow diagram used to calculate the steady-state concentrations of different species by means of the dispersion model.

inhibit or promote the ozone decomposition in free radicals. Following results shown in Fig. 2 it is deduced that water taken from the river Gevora contains substances, carbonates among others, that scavenge the action of hydroxyl radicals. This results in a partial inhibition of the oxidation rate. On the contrary, water from Cordobilla reservoir likely contains other substances that promote the ozone decomposition and increase the oxidation rate of atrazine. As can also be observed from Fig. 2 the kinetic model reproduces reasonably well the experimental time concentration profiles although some deviations are noted regarding the ozonation with Cordobilla water, mainly once the steady state has been reached.

On the other hand, Fig. 2 also shows the simulation results obtained when the dispersion model is applied. With this model, however, only results corresponding to the stationary state were calculated. As can be seen, calculated concentrations are also close to the experimental ones as in the tanks in series model.

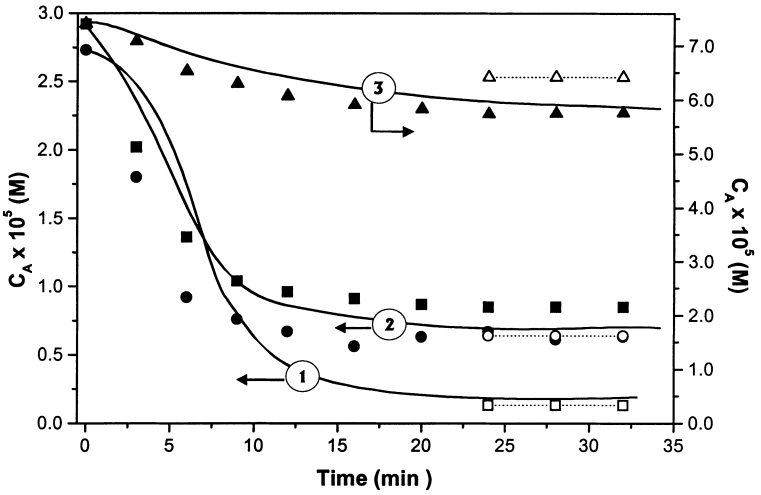

Fig. 2. Ozonation of atrazine in natural waters. Evolution of atrazine concentration with time. Conditions: pH = 8.5, T = 293 K, contactor (I), ozone dose = 6.65×10^{-5} M. Water type: (●, ○, 1) ultrapure water; (□, ■, 2) Cordobilla reservoir water; (▲, △, 3) Gevora river water. Solid symbols: experimental results; solid numbered lines: tanks in series model; dotted lines plus open symbols: steady state concentrations; dispersion model.

Finally, Fig. 3 presents results of calculated concentrations of the ozonation intermediates considered in the kinetic model. As can be seen the dispersion model predicts concentrations of DEA and DIA, first intermediates, higher than those from the tanks in series model. Notice that experimental concentrations of intermediates were not determined in this work because of some analytical problems arising when using the HPLC

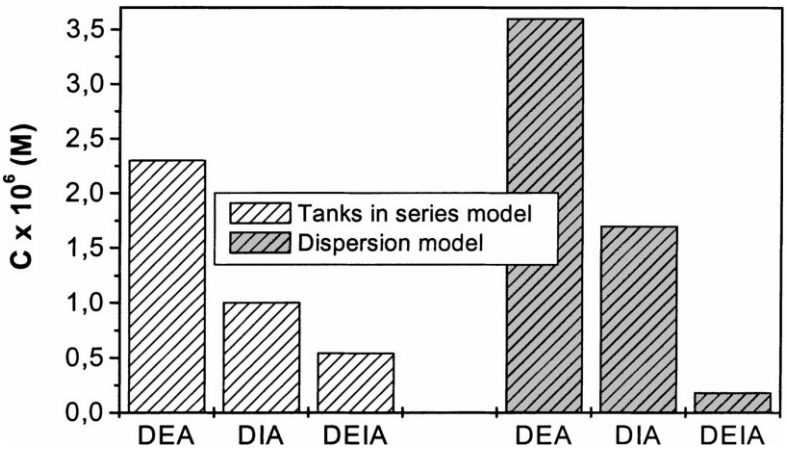

Fig. 3. Atrazine ozonation in Cordobilla reservoir water. Calculated concentrations of DEA, DIA and DEIA at steady state regime. Conditions as in Fig. 2.

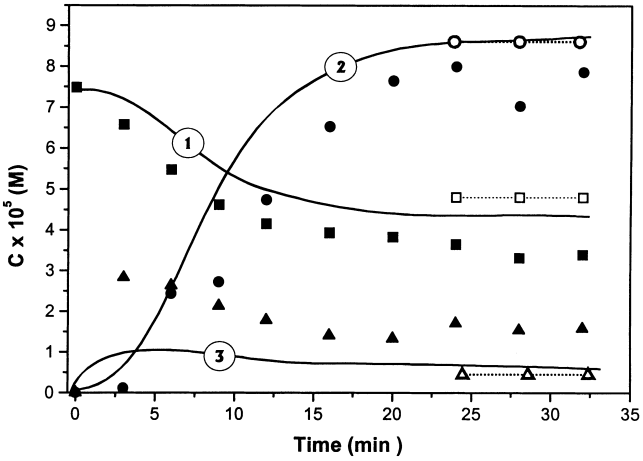

Fig. 4. O_3/H_2O_2 oxidation of atrazine in Gevora river water. Atrazine, dissolved ozone and hydrogen peroxide concentration profiles with time. Conditions: pH = 7.0, $T = 293$ K, contactor (II), ozone dose = 4.83×10^{-5} M, H_2O_2/O_3 ratio = 0.31 g/g. (□, ■, 1) Atrazine; (●, ○, 2) hydrogen peroxide; (▲, △, 3) dissolved ozone. Solid symbols: experimental results; solid numbered lines: tanks in series model; dotted lines plus open symbols: steady state concentrations; dispersion model.

equipment. These types of problems have also been found in other works to follow the kinetics of formation and disappearance of by-products of the oxidation of pesticides [21].

3.2.2. Ozone combined with hydrogen peroxide

Combination of ozone with hydrogen peroxide as shown in the mechanism above is a possible route to produce hydroxyl radicals and therefore, to increase the oxidation rate of herbicides like atrazine and its metabolites. In this work, some experiments of ozone combined with hydrogen peroxide were also carried out in the non-photochemical contactor in order to test the validity of the kinetic model. Fig. 4 shows, as an example, some of the results obtained. In this case, experimental and calculated (from the tanks in series model) concentrations of atrazine, hydrogen peroxide and dissolved ozone are plotted versus reaction time for one experiment carried out with water from the river Gevora. Also, it is shown the concentrations calculated from the dispersion model at steady state. Before commenting on the simulation results, it can be noted that conversion of atrazine was improved compared to that achieved from ozonation alone. As far as the simulation is concerned, on the other hand, it can be noticed that calculated concentrations (from the tanks in series model) are close to the experimental ones at any given time. The dispersion model predicts, however, steady state concentrations of remaining atrazine slightly higher than those calculated from the tanks in series model.

With respect to the intermediate concentrations, Fig. 5 shows some examples of the calculated results obtained. It can be seen that calculated concentrations are of the same order of magnitude as those predicted for ozonation alone, although this also depends on the type of water.

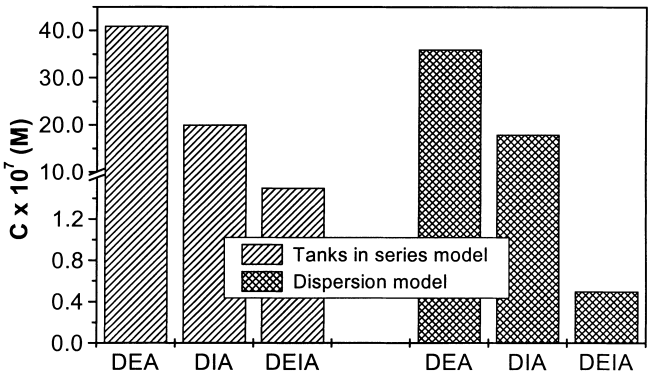

Fig. 5. O_3/H_2O_2 oxidation of atrazine in Gevora river water. Calculated concentrations of DEA, DIA and DEIA at steady state regime. Conditions as in Fig. 4.

3.2.3. Ozone combined with UV radiation

Finally, a series of experiments of ozone combined with 254 nm UV radiation were also completed. This oxidising system presents at least three ways to initiate the generation of free radicals (reactions (11) to (14)), although reaction (12) is the most important one [12]. Figs. 6 and 7 show the evolution of experimental and calculated (from the tanks in series model) concentrations of atrazine, hydrogen peroxide and dissolved ozone with time together with calculated results at steady state. These results were obtained from the dispersion model and correspond to two O_3/UV oxidation experiments carried out with

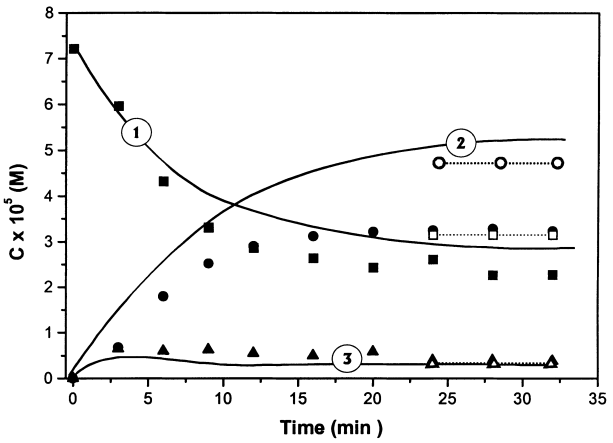

Fig. 6. O_3/UV oxidation of atrazine in Gevora river water. Atrazine, dissolved ozone and hydrogen peroxide concentration profiles with time. Conditions: pH = 7.0, $T = 293$ K, contactor (I), ozone dose = 6.81×10^{-5} M, $I_0 = 1.9 \times 10^{-6}$ Einstein l^{-1} s^{-1}), $L = 6.6$ cm. (□, ■, 1) Atrazine; (●, ○, 2) hydrogen peroxide; (▲, △, 3) dissolved ozone. Solid symbols: experimental results; solid numbered lines: tanks in series model; dotted lines plus open symbols: steady state concentrations; dispersion model.

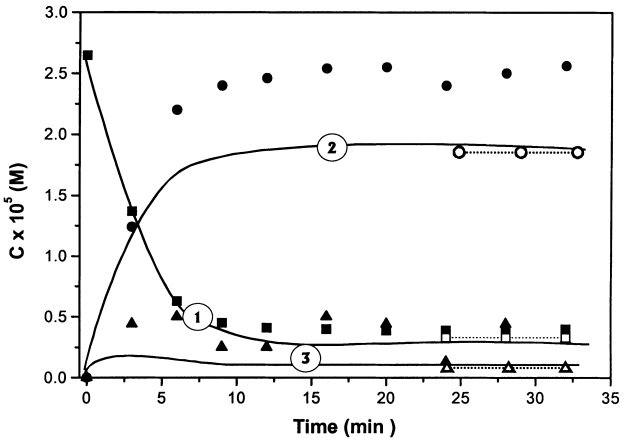

Fig. 7. O_3/UV oxidation of atrazine in Cordobilla reservoir water. Atrazine, dissolved ozone and hydrogen peroxide concentration profiles with time. Conditions: pH = 8.5, $T = 293$ K, contactor (I), ozone dose $= 6.81 \times 10^{-5}$ M, $I_0 = 1.9 \times 10^{-6}$ Einstein l^{-1} s^{-1}, $L = 6.6$ cm. (□, ■, 1) Atrazine; (●, ○, 2) hydrogen peroxide; (▲, △, 3) dissolved ozone. Solid symbols: experimental results; solid numbered lines: tanks in series model; dotted lines plus open symbols: steady state concentrations; dispersion model.

Gevora and Cordobilla waters. Comparing Fig. 6 to Figs. 2 and 4, it can be observed that the ozone–UV process led to the highest atrazine conversion among the ozonation processes studied. Conversion of atrazine in Cordobilla water was higher than that in river Gevora which coincides with results shown in Fig. 1. This also confirms the presence of scavenging substances in water from river Gevora or substances that promote ozone decomposition in water from Cordobilla reservoir. Concerning the simulation itself, both models lead to calculated concentrations similar to those determined experimentally. The main deviations are observed in predicting the concentration of hydrogen peroxide in the case of ozonation with water from Cordobilla reservoir. Notice the low concentration of dissolved ozone achieved which is likely due to ozone photolysis reactions both in gas and water phases.

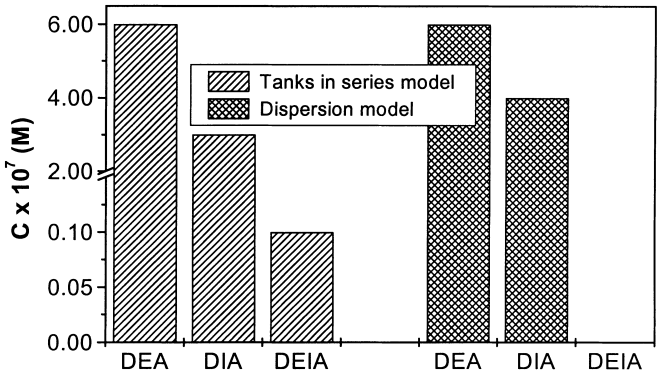

Fig. 8. O_3/UV oxidation of atrazine in Gevora river water. Calculated concentrations of DEA, DIA and DEIA at steady state regime. Conditions as in Fig. 6.

Fig. 8, on the other hand, presents the calculated concentrations of intermediates predicted from both kinetic models applied once the steady state is reached. The most singular result is that the concentration of intermediates is about one order of magnitude lower than that predicted for the other two ozonation processes studied. Also, it should be noticed that the dispersion model predicts no concentration of DEIA at steady state. These results are noteworthy since they suggest the ozonation combined with UV radiation, as an oxidation process, is more effective than the two other ozonations studied to remove atrazine and intermediates from water. This also supports the free radical character of the ozonation processes.

4. Conclusions

The fate of atrazine and its first intermediates formed during its advanced chemical oxidation with ozone, hydrogen peroxide and/or UV radiation in water has been simulated with the use of kinetic models. These models have been deduced from a mechanism of reactions and have involved the acquisition of mass transfer, chemical and photochemical rate data and non-ideal flow analysis through the contactors used.

Two different kinetic systems have been applied based on the tanks in series and dispersion non-ideal flow models. The kinetic models yield similar calculated concentrations of atrazine, hydrogen peroxide and dissolved ozone, with main differences observed in concentrations of intermediate compounds. Also, the models predict reasonably well the experimental remaining concentrations of the aforementioned three compounds. Therefore, due to its mathematical simplicity the tanks in series model results specially recommended versus the kinetic system based on the dispersion model. Furthermore, the tanks in series model allows for the study of the non-stationary chemical oxidation until steady state conditions are reached.

The kinetic models confirm that advanced oxidation of atrazine is mainly due to free radical reactions involving the participation of hydroxyl radicals. Also, they allow the most suitable advanced chemical oxidation to be chosen, which in this case resulted to be the O_3/UV system.

As far as oxidation rate of atrazine is concerned, knowledge of ozone decomposition rate data in the water used is fundamental to establish the inhibiting or promoting character of the water. Thus, the kinetic models predict that the fastest oxidation rates are achieved in water from Cordobilla reservoir which comports the fact that this water presents the highest $k_{in}C_{in}$ value.

It can be finally concluded that the kinetic model presented in this work can be used with appropriate mass transfer, chemical rate and non-ideal flow data to simulate the performance and efficiency of the (ozone, hydrogen peroxide and UV radiation) advanced chemical oxidation of other priority pollutants of water.

List of symbols

C_g	ozone concentration in the gas phase (M)
C_i	concentration of species i in water (M)
$C^*_{O_3}$	ozone concentration at the gas–water interface (M)
C_{O_3gi}	ozone concentration of the gas entering the reactor (M)

C_{O_3gs} ozone concentration of the gas leaving the reactor (M)
dh differential height in the contactor (m)
D_i diffusivity of species i in water ($m^2\ s^{-1}$)
F_i fraction of absorbed radiation that compound i absorbs (dimensionless)
H total height of liquid in the contactor (m)
He constant of Henry for the ozone–water system ($Pa\ l\ mol^{-1}$)
I_0 intensity of incident radiation ($Einstein\ l^{-1}\ s^{-1}$)
k_C constant defined in Eq. (42)
$k_{D,i}$ rate constant of the direct reaction between ozone and the species i ($M^{-1}\ s^{-1}$)
k_H constant defined in Eq. (43)
$k_{OH,i}$ rate constant of the reaction between hydroxyl radicals and the species i ($M^{-1}\ s^{-1}$)
k_S constant defined in Eq. (41)
k_L individual liquid side mass transfer coefficient ($m\ s^{-1}$)
k_La volumetric mass transfer coefficient (s^{-1})
k_{ti} radical termination rate ($M^{-1}\ s^{-1}$)
L effective path of incident radiation through the photoreactor (cm)
N number of perfectly mixed tank reactors
N_{O_3} ozone absorption rate ($M\ s^{-1}$)
Pe_L Peclet number in the water phase, defined by Eq. (62)
Q flow rate ($m^3\ s^{-1}$)
r_i reaction rate of any ozone involving reaction (s^{-1})
r_{UVi} rate of the photolysis of species i ($M\ s^{-1}$)
R constant of perfect gases ($Pa\ l\ mol^{-1}\ K^{-1}$)
S transversal section of the contactors (m^2)
t time (s)
T temperature (K)
u superficial velocity of water ($m\ s^{-1}$)
V contactor volume (m^3)
z_{DE} stoichiometric coefficient of reaction (1), moles of atrazine consumed per mole of ozone consumed to form deethylatrazine (dimensionless)
z_{DI} stoichiometric coefficient of reaction (2), moles of atrazine consumed per mole of ozone consumed to form deisopropylatrazine (dimensionless)
z_{RE} stoichiometric coefficient of reaction (25), moles of deethylatrazine formed per mole of atrazine consumed (dimensionless)
z_{RI} stoichiometric coefficient of reaction (26), moles of deisopropylatrazine formed per mole of atrazine consumed (dimensionless)

Greek letters

β liquid fraction in the contactor
ε_i extinction coefficient of species i in water ($M^{-1}\ cm^{-1}$)
Φ_i quantum yield at 254 nm of species i ($mol\ photon^{-1}$)
λ normalised height fraction of contactors, defined in Eq. (61) (dimensionless)
σ^2 variance of the residence time distribution function (min^2)

τ hydraulic time (min)
ω_j reaction rate of any *j* chemical species involving reaction as a function of parameters ψ_{O_3}, ψ_i and rate constants ($M\,s^{-1}$)
ω_{O_3} reaction rate of any ozone involving reaction as a function of parameters ψ_{O_3}, ψ_i and rate constants ($M\,s^{-1}$)
ξ_j function defined in Eq. (64)
ξ_{O_3} function defined in Eq. (63)
ψ_g normalised concentration of ozone in the gas phase, defined in Eq. (58) (dimensionless)
ψ_i normalised concentration of species *i*, defined in Eq. (60) (dimensionless)
ψ_{O_3} normalised concentration of ozone in water, defined by Eq. (59) (dimensionless)

Acknowledgements

We thank the CICYT of Spain for its economic support (Research Project AMB97/339).

References

[1] G. Reynolds, N. Graham, R. Perry, R.G. Rice, Ozone Sci. Eng. 11 (1989) 339.
[2] C.D. Adams, S.J. Randtke, E.M. Thurman, R.A. Hulsey, in: 109th Annual Conference Proceedings of American Water Works Association, Cincinnati, OH, 1990, pp 1–24.
[3] J.M. Sayre, J. Am. Water Works Assoc. 80 (1988) 53.
[4] F.J. Beltrán, J.F. García-Araya, P. Alvarez, F.J. Rivas, J. Chem. Technol. Biotechnol 71 (1998) 345.
[5] B. Legube, S. Guyon, M. Doré, Ozone Sci. Eng. 9 (1987) 233.
[6] M. Prados, H. Paillard, P. Roche, Ozone Sci. Eng. 17 (1992) 183.
[7] C.D. Adams, S.J. Randtke, Environ. Sci. Technol. 26 (1992) 2218.
[8] F.J. Beltrán, J.F. García-Araya, B. Acedo, Water Res. 28 (1994) 2153.
[9] F.J. Beltrán, J.F. García-Araya, B. Acedo, Water Res. 28 (1994) 2165.
[10] A. Laplanche, R. Bastiment, V. Boisdon, in: Proceedings of the 1st Research Symposium on Les sous-produits de traitement et d'epuration des eaux, 29-1-29-19, Poitiers, France, 1994.
[11] F.J. Beltrán, G. Ovejero, B. Acedo, Water Res. 27 (1993) 1013.
[12] F.J. Beltrán, Ozone Sci. Eng. 21 (1999) 207.
[13] H.S. Fogler, Prentice-Hall, Englewood Cliffs, New Jersey, 1989.
[14] B. Langlais, D.A. Reckhow, D.R. Brink, (Eds.), Lewis Publishers, Chelsea, MI, USA, 1991.
[15] H. Bader, J. Hoigné, Water Res. 15 (1991) 449.
[16] R.A. Lazrus, G.L. Kok, S.N. Gitlin, J.A. Lin, S.E. McLaren, Anal. Chem. 87 (1985) 917.
[17] P.S.V. Danckwerts, MacGraw-Hill, New York, 1970.
[18] S. Staehelin, J. Hoigné, J. Environ. Sci. Technol. 19 (1985) 1206.
[19] F.J. Beltrán, M. González, F.J. Rivas, P. Alvarez, Environ. Toxicol. Chem. 15 (1996) 868.
[20] S. Morooka, K. Kusakabe, J. Hayasi, K. Isomura, K. Ikemizu, Ind. Eng. Chem. Res. 27 (1988) 2372.
[21] S. Chiron, A.R. Fernández-Alba, A. Rodriguez, Trac-Trend. Anal. Chem. 16 (1997) 518.